

Human remains from Tappeh Khatoonlar, Iran, 2019

Mohammadreza Nemati¹, Pegah Goodarzi^{*2}, Hasan Nami³,
Mehdi Mousavina³

¹ Iranian Center for Archaeological Research,
30 Tir St., Imam Khomeini Avenue, Tehran, Iran

² Department of Archaeology, Simon Fraser University, Burnaby, BC V5A 1S6, Canada
email: Pegah_Goodarzi@sfu.ca (corresponding author)

³ Department of Archaeology, University of Neyshabur,
Adib Blvd., Neyshabur, Khorasan Razavi, Iran

Tappeh Khatoonlar (35°41'41"N, 50°47'46"E) is a historical mound in the center of Mehrdasht, a village in Malard city, Tehran Province of Iran (Figure 1). In May 2019, Mohammadreza Nemati and his team excavated the site to define the boundaries and core zones (Nemati 2019). As a result of their work, remains of a significant architectural complex were unearthed (Figure 2). Relative dating based on the coins, pottery, and architectural styles shows that this complex was built during the Seljuk period (mid-11th century to the late 12th century CE) and was in use until the Ilkhanate period (mid-13th century to the mid-14th century CE). The building was abandoned around the end of the Ilkhanate period, and its ruins were used as a graveyard until the early Qajar period (1789–1925 CE) (Nemati 2019).

In total, 11 graves were excavated in trenches dug northeast and southeast of the mound. All individuals were buried in simple pits on their right side, facing the Qiblah, their heads toward the northwest and feet toward the southeast. Due to the contemporary destruction of the mound, some graves were disturbed, and some parts of the skeletons were missing (Nemati 2021).

Osteological analysis of human remains retrieved from Tappeh Khatoonlar was done in August 2023 based on the standard protocols presented in Buikstra and Ubelaker (1994). For adult individuals, sex was assessed mainly based on the morphology of the os coxae and the skull. For this purpose, the ventral arch, subpubic concavity, ischiopubic ramus ridge, greater sciatic notch, preauricular sulcus in the hip bone, as well as the nuchal crest, mastoid process, supraorbital margin, glabella, and mental eminence in the skull were examined. Examinations were conducted using the methodologies outlined by Buikstra and Ubelaker (1994), and Ferembach (1980). Age at death was estimated based on the morphology of the pubic symphysis. Scoring was undertaken based on the system provided by Todd (1920), Brooks and Suchey (1990), and the morphology of the auricular surface (Lovejoy 1985). The development and eruption status of teeth (AlQahtani et al. 2010), diaphyseal length, and

epiphysis fusion status (Schaefer et al. 2009) were the basis of age-at-death estimation for the subadult individual. Pathological conditions, including degenerative joint disease, were also diagnosed (Waldron 2008). Dental carious lesions were scored according to their location on the tooth's anatomical structure and their position on the

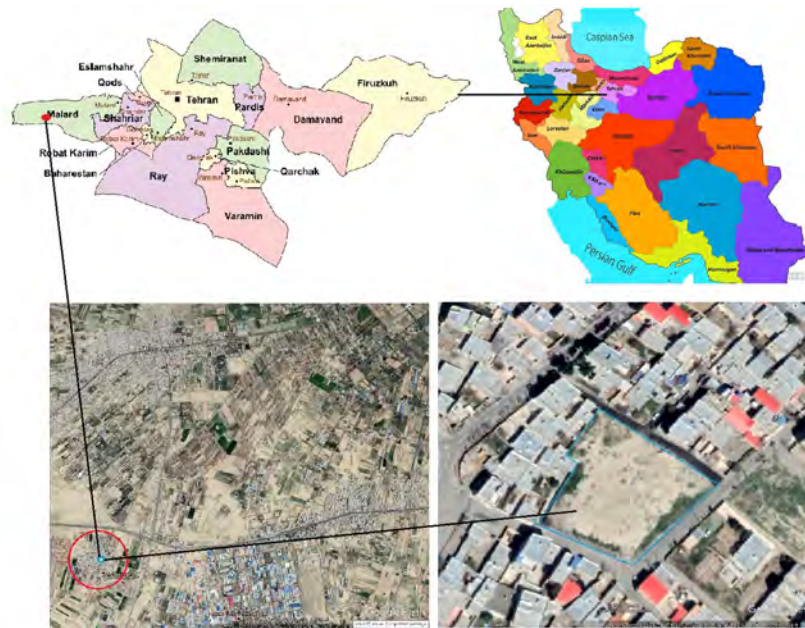


Figure 1. The site's location on Iran's map and Malard city. Drawing by Mohammadreza Nemati.

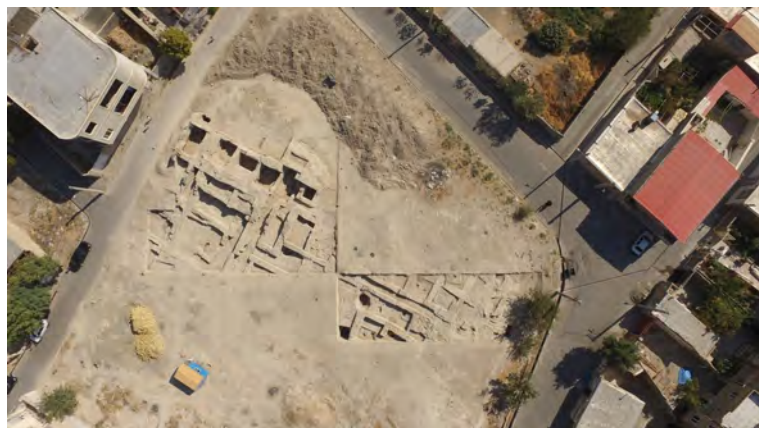


Figure 2. Aerial view of the site during excavation. Photograph by Mohammadreza Nemati.

Table 1. General characteristics of human remains from Tappeh Khatoonlar. The asterisks mark less probable assessments.

Trench	Feature	Sex	Age at death	Completeness
F6	100	?	6 months	skull bones + partially preserved body
F6	106	?	adult	a right-side humerus
F6	109	M	36-44	almost complete
F6	117	M	30-40	lower extremity
F7	112	M	36-40	almost complete
G4.A	no tag	M	adult	skull + fragmented postcranial bones
G4.B	no tag	?	adult	a right-side humerus
G5	100	?	adult	incomplete postcranial skeleton
G5	133.A	M*	adult	cranial vault+ mandible+ fragmented mixed bones
G5	133.B	?	adult*	right mandibular condyle
G5	101	M*	30-40	cranium+ incomplete postcranial skeleton
H4	102	?	adult	fragmented elements
H4	106	M	40-44	almost complete
H5	108.A	M*	40-44	complete
H5	108.B	?	adult	a fibula
no tag	no tag	M	35-45	fairly complete

Table 2. Dental health of human remains from Tappeh Khatoonlar. AMTL: antemortem tooth loss, LEH: linear enamel hypoplasia, DC: dental calculus.

Trench	Feature	Caries	AMTL	Abscess	LEH	DC
F6	109	3/13	8/32			
F7	112	4/11	2/32	alveolar bone loss and root exposure		
G4.A	no tag	0/4	1/32			
G5	100	0/3				
G5	133.A	0/7	6/32	alveolar bone loss		slight
G5	101	0/3	1/32			
H4	102	0/4			2	moderate
H4	106	10/21	7/32		4	moderate
H5	108.A	3/6	21/32	alveolar bone loss and root exposure		slight
no tag	no tag	1/7	21/32			

tooth surface (Hillson 1996; Steckel et al. 2005). Linear enamel hypoplasia (Brickley & McKinley 2004) and the size of dental calculus deposits (Brothwell 1981) were also recorded.

The minimum number of individuals is 16, including an infant, 9 male individuals, and skeletal elements from 6 adults of unknown sex (Table 1). The age at death for adult individuals falls mostly within the 30–45 year range, based on the morphological changes of the pubic symphyses and auricular surfaces. Because reliable pelvic indicators were not preserved in all individuals, this age range may under-represent both younger and older adults. Overall, the human remains were remarkably well-preserved, allowing for a detailed pathological assessment.

This skeletal assemblage indicates generally poor dental health among adults (Table 2). Antemortem tooth loss (AMTL) was recorded in 8 individuals from whom max-

illae and/or mandibles were preserved. Two individuals (H5/108 and NT) exhibited extensive loss (over half of the dentition missing and alveolar bone remodeled), while several others (e.g., F6/109, H4/106) showed moderate tooth loss. In individual H5/108, the jaws were entirely edentulous with complete alveolar fusion (Figure 3). Individual F7/112 displayed extensive maxillary tooth loss accompanied by multiple dental abscesses and severe caries. Dental caries is the result of localized enamel demineralization due to acidic byproducts secreted by a polymicrobial biofilm (Ullinger et al. 2023). In this assemblage, 5 people had dental caries, ranging from minor surface damage and small cavities to deep coronal cavities. In individual H4/106, the highest number of carious lesions was observed, mainly on the mesial surfaces of the premolars and molars in both maxillary and mandibular teeth. Horizontal bone loss associated with periodontal disease in the right-side maxilla has also caused alveolar bone resorption and root exposure extending from RC¹ to RM³ in this individual.

Dental abscess or periapical infection develops when inflammation in the root canal allows pathogens to emerge from the apical foramen, triggering an inflammatory response in periodontal tissues and leading to a periapical granuloma (Hillson 1996). Dental abscess was observed in three individuals from the assemblage. In individual H5/108.A, dental abscesses and horizontal absorption of alveolar bone resulted in the AMTL, and tooth roots were exposed in the mandible and maxilla.

Calculus is a mineralized plaque attached to the tooth's surface, derived from saliva (Hillson 1996). Four individuals from this assemblage had dental calculus, ranging from slight to medium deposits, on the incisors, premolars, and molars' lingual, labial, and buccal surfaces.



Figure 3. Edentulous and atrophied maxillary arch of individual H5/108. Photograph by Pegah Goodarzi.

Two individuals also showed evidence of linear enamel hypoplasia (LEH) resulting from episodic growth disruption during their childhood. LEH was observed as slight single lines on RI₁ and RP₂ in individual H4/102 and multiple slight lines on RP₁, RP₂, RC¹, and RP² in individual H4/106.

Bone diseases were highly prevalent in the form of degenerative joint disease (DJD) affecting the spine and non-spinal joints. In the case of spinal DJD, the most advanced stages of spondylosis associated with severe osteophytes were observed in individuals G5/100 and F7/112. In individual G5/100, all 5 lumbar vertebrae and the first segment of the sacrum exhibited pitting on the surface and severe marginal osteophytes (Figure 4). The same conditions were observed in lumbar vertebrae 2 to 5 in individual F7/112. In addition, Schmorl's nodes were recorded in the inferior-superior surfaces of lumbar vertebrae 4 and 5, respectively. Furthermore, several cases of spondylosis, osteophytes, and Schmorl's nodes were recorded in five other individuals. Non-spinal DJD was also common in this assemblage. Individual G5/100 showed

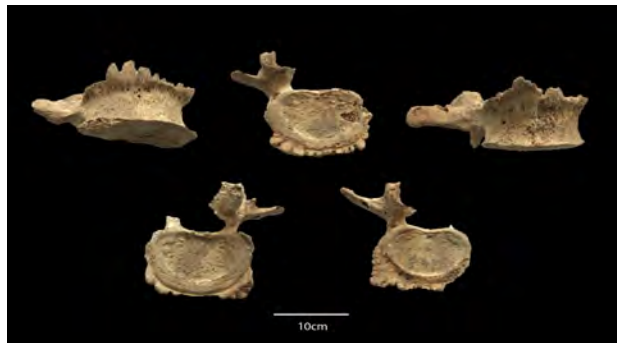


Figure 4. Severe marginal osteophyte in the lumbar vertebrae of individual G5/100.
Photograph by Pegah Goodarzi.



Figure 5. Pitting on the auricular surface of the ilium in individual F7/112. Photograph by Pegah Goodarzi.

several instances of joint lipping, osteophytes, and pitting on the radial tuberosity of the right radius, the head of the first left metatarsal, the proximal end of the fifth left metatarsal, as well as the head of the first metacarpal of an unknown side. In G5/133.A, osteophytes and lipping were recorded in the distal epiphysis of the right radius, and pitting was present at the distal radial articular surface. An osteophyte was observed in the radial head of the same side. The left talus from the same individual was recorded with severe lipping and osteophytes in its articular surfaces. In individual F7/112, osteoarthritis with marginal osteophytes was noted on the distal condyle of the right femur and the proximal epiphysis of the right tibia. The same condition was observed in the distal epiphyses of the left and right humeri. Lipping was also seen in the coronoid process of the ulna and the radial head on the right side. Additionally, porosity was present at the lateral ends of both clavicles. Pitting was also noted on the auricular surface of the ilium on both sides (Figure 5). Osteoarthritis associated with severe lipping was also noted in the proximal epiphysis of the left tibia in individual G4. A. Lipping and osteophytes were also recorded in the sacroiliac joints of individual F6/117. In this individual, lipping in the posterior facet of the right calcaneus and severe osteoarthritis in the proximal epiphysis of the left tibia were also observed. Lipping at the radial tuberosity was also observed in the NT individual's left radius. Osteophyte and bone porosity were present on the first metatarsals from both sides in this individual. In individual H5/108, porosity, irregular joint surface, and bone spurs were observed in the distal and proximal epiphyses of the left fibula, which may indicate osteoarthritis. In addition, new bone formation was recorded in the sternal end of the (probably) 6th rib.



Figure 6. Bone spurs on the calcaneal tubers of individual F6/117. Photograph by Pegah Goodarzi.

Bone spurs were present on the calcaneal tuberosity at the insertion point of the Achilles tendon in 5 out of 10 individuals with preserved calcanei from this assemblage (Figure 6). In the NT individual, single rib spurs were observed on the ventral side of the 10th ribs at both sides. In addition, in individual F6/117, a bone spur was observed at the lateral side of the distal epiphysis of the right tibia. Also, in individual G5/100, bone spurs were present on both patellae, on the anterior and proximal aspects, where the quadriceps tendon attaches to the patella. Three ribs from individual F6/109 show callus formation on the ventral aspect of the ribs, consistent with partially healed fractures that were extended transversely through the rib shafts. The exact rib numbers are uncertain, but their morphology suggests a mid-thoracic position (around ribs 5–8). No additional traumatic lesions were observed elsewhere in the assemblage.

In conclusion, the skeletal assemblage from Tappeh Khatoonlar was overrepresented by male individuals. While most skeletons in the collection are adults, the presence of a child suggests that the graveyard may not have been exclusively designated for adults. Stress markers and traumatic lesions among this group of individuals were low. Still, the prevalence of dental and skeletal pathologic conditions might suggest a diet abundant with fermentable sugar and occupations that impose high mechanical strains on the skeleton.

References

AlQahtani S., Hector M.P., Liversidge H.M. (2010), *The London atlas of human tooth development and eruption*, American Journal of Physical Anthropology 142(3):481-490.

Brickley M., McKinley J.I. (2004), *Guidelines to the standards for recording human remains*, Southampton & Reading: BABAO, University of Southampton.

Brooks S., Suchey J.M. (1990), *Skeletal age determination based on the os pubis: A comparison of the Acsádi-Nemeskéri and Suchey-Brooks methods*, Human Evolution 5(3):227-238.

Brothwell D.R. (1981), *Digging up bones: The excavation, treatment, and study of human skeletal remains*, Ithaca: Cornell University Press.

Buikstra J.E., Ubelaker D.H. (eds.) (1994), *Standards for data collection from human skeletal remains*, Fayetteville: Arkansas Archaeological Survey Research.

Ferembach D. (1980), *Recommendations for age and sex diagnosis of skeletons*, Journal of Human Evolution 9:517-549.

Hillson S. (1996), *Dental anthropology*, Cambridge: Cambridge University Press.

Lovejoy C.O. (1985), *Dental wear in the Libben population: Its functional pattern and role in the determination of adult skeletal age at death*, American Journal of Physical

Anthropology 68(1):47-56.

Nemati M.R. (2019), *Excavation and site management of Tappeh Khatoonlar, Mehrdasht Malard*, unpublished report, Tehran: Archaeological Research Institute.

Nemati M.R. (2021), *The report of a rescue excavation in Tappeh Khatoonlar, Mehrdasht, Malard* [in:], “The 18th Annual Meeting of Iranian Archeology”, R. Shirazi (ed.), Tehran: National Museum of Iran Press, pp. 855-857.

Schaefer M., Black S., Scheuer L. (2009), *Juvenile osteology: A laboratory and field manual*, San Diego: Academic Press.

Steckel R., Larsen C., Sciulli P., Walker P. (2005), *The Global History of Health Project data collection codebook*, Columbus: Ohio State University.

Todd T.W. (1920), *Age changes in the pubic bone. I. The male white pubis*, American Journal of Physical Anthropology 3(3):285-334.

Ullinger J., Loewen T., Grauer A.L. (2023), *Dental disease* [in:] “The Routledge handbook of paleopathology”, A.L. Grauer (ed.), London & New York: Routledge, pp. 360-378.

Waldron T. (2008), *Palaeopathology*, Cambridge: Cambridge University Press.